Electrochimica Acta 56 (2011) 2299–2305

Contents lists available at ScienceDirect

Electrochimica Acta

journal homepage: www.elsevier.com/locate/electacta

Palladium-based electrodes: A way to reduce platinum content in polymer electrolyte membrane fuel cells

Ermete Antolini[a,b,*], Sabrina C. Zignani[b], Sydney F. Santos[c], Ernesto R. Gonzalez[b]

[a] Scuola di Scienza dei Materiali, Via 25 aprile 22, 16016 Cogoleto, Genova, Italy
[b] Instituto de Química de São Carlos, USP, C. P. 780, São Carlos, SP 13560-970, Brazil
[c] CECS - UFABC, Rua Santa Adélia, 166, Santo André - SP, Brazil

ARTICLE INFO

Article history:
Received 27 August 2010
Received in revised form
27 November 2010
Accepted 30 November 2010
Available online 8 December 2010

Keywords:
PEMFC
Palladium
PdPtCo/C catalyst
Hydrogen oxidation
Oxygen reduction

ABSTRACT

To decrease the Pt content, a polymer electrolyte membrane fuel cell (PEMFC) was formed using a carbon supported $Pd_{96}Pt_4$ catalyst as the anode material, and a carbon supported $Pd_{49}Pt_{47}Co_4$ catalyst as the cathode material. The as-obtained Pd-based PEMFC with an overall Pd:Pt:Co atomic composition of electrodes (anode + cathode) = 72:26:2 exhibited a performance not too far from that of the fuel cell with the conventional 100% Pt electrodes. With a Pt content of 35 wt% of that of the cell with full Pt electrodes, at a current density of 1 A cm^{-2} the performance loss of the cell with the Pd-based catalysts was only 11%, with 6% ascribed to the anode catalyst and 5% to the cathode catalyst. The maximum power density of the Pd-based cell was 76% of that of the cell with Pt catalysts.

1. Introduction

Recently, high operating efficiency and environmental friendliness polymer electrolyte fuel cells (PEMFCs) have begun to move from the demonstration phase to commercialization due to the impressive research effort in recent years. Nevertheless, several outstanding cost reduction problems and technological challenges remain to be solved. Among the technological challenges in terms of PEMFC electrodes, the development of anode electrocatalysts tolerant to carbon monoxide and cathode electrocatalysts able to reduce the overpotential encountered under open circuit conditions and significantly enhance the exchange current density are the most significant. One of the barriers to commercialization remains the prohibitive cost of this technology. The U.S. Department of Energy set long-term goals for PEMFC performance in a 50 kW stack that included operation with cathode loadings of 0.05 mg cm^{-2} or less of precious metals [1]. The limited supply and high cost of the Pt used in PEMFC electrocatalysts necessitate a reduction in the Pt level. Generally, there are two ways to reduce the use of Pt in PEMFCs, that is (1) Pt electrodes with low Pt content and (2) total or partial substitution of Pt with other metals. In the former case, as discussed by Wee et al. in a recent review [2], the reduction of Pt loading in electrocatalysts can be achieved through an enhancement of the Pt utilization by increasing the active Pt sites, thinning the active layer thickness and introducing smaller, carbon-supported, nanometer-sized, Pt particles. Regarding the point (2), the partial or total substitution of platinum with palladium seems a promising way to reduce Pt content [3]. Pt and Pd have very similar properties (same group of the periodic table, same fcc crystal structure, similar atomic size). The cost of palladium is about three times lower than that of platinum, so it could be a good substitute for Pt as electrode catalyst in fuel cells. Moreover, Pd is interesting as it is at least fifty times abundant on the earth than Pt. Pd, as other platinum-group metals, presents electrocatalytic activity for both the hydrogen oxidation reaction (HOR) and the oxygen reduction reaction (ORR), but the HOR and ORR activities of Pd are considerably lower than those of Pt [4–6]. The performance of Pd/C for the HOR as anode catalyst in PEMFC is very poor [7,8]. It has be found, however, that by addition of a very low amount (5–10 at.%) of Pt, the HOR activity of Pd attains that of pure Pt [8,9]. On the other hand, it has been reported that by addition of a suitable metal, as Co and Fe, the ORR activity of Pd becomes comparable to that of Pt [10–13]. The activity of these Pt-free Pd-based catalysts, however, seems to depend on the synthesis method. Indeed, in various papers a considerably lower ORR activity of Pd-based catalysts than Pt was also reported [14–16]. Raghuveer et al. [14] found that, in the absence of thermal treatment, the ORR activity of Pd–Co–Au/C, prepared

* Corresponding author at: Scuola di Scienza dei Materiali, Department of Chemistry, Via 25 aprile 22, 16016 Cogoleto, Genova, Italy.
E-mail address: ermantol@libero.it (E. Antolini).

0013-4686/$ – see front matter © 2010 Elsevier Ltd. All rights reserved.
doi:10.1016/j.electacta.2010.11.101

both by the borohydride method and the reverse microemulsion method, was lower than that of Pt/C. Wang et al. [15] found the ORR overpotential on all of Pd–Co/C electrocatalysts with different Pd/Co atomic ratios prepared by a modified polyol reduction is higher than that on the Pt/C catalyst, indicating that the ORR activity on Pd-based catalysts is lower than that on the Pt-based catalysts in pure acidic solution. Finally, Liu and Manthiram [16] observed that the as-prepared Pd_4Co/C catalyst, synthesized by a modified polyol reduction process, has lower catalytic activity for ORR than the as-prepared Pt/C, although all of them have a similar particle size.

The addition of Pt is another way to increase the ORR of Pd. Indeed, many works showed that platinum addition increases the ORR activity of palladium [17–23] and that the dependence of the ORR activity on the Pt content goes through a maximum. In particular, Guerin et al. [21] and Ye and Crooks [22] reported an increase in the activity of Pd with the amount of Pt, following a parabolic trend with a maximum activity in the composition range of 50–90% Pt that is potential-dependent. The presence of platinum should improve the stability of palladium in acid media as well as reinforce the electrocatalytic activity for the ORR through the synergistic effects of the metals.

Generally the particle size of carbon supported metals increases going from Pt to Pt–Pd to Pd, independently of the preparation method [8,17,24–27]. The increase in metal particle size is more significant for Pd contents >50 at.%. The different dispersion of the metal nanoparticles on the carbon support is mainly due to their different nucleus-growth mechanisms of metal nanoparticles in Pt/C and Pd/C catalysts. Recently Beard et al. [28] used surface modification of a carbon support preceding deposition of catalytic Pd seed nuclei to prepare Pt–Pd catalysts by the electroless deposition (ED) of Pt onto the Pd surface. Functionalization of a carbon support with nitric acid to form surface carboxylic acid groups is followed by pre-treatment in a pH 14 bath to convert the acid moieties to the corresponding carboxylate ($RCOO^-$) groups. The negative surface charge results in an electrostatic attraction between the carboxylate groups and positively charged Pd^{2+} cations during wet impregnation to produce smaller catalytic Pd seed nuclei which act as deposition sites for Pt in the ED process. Using this method Ohashi et al. [23] prepared various Pd–Pt/C catalysts with a maximum Pd/Pt atomic ratio of *ca.* 1 and a maximum metal (Pd + Pt) loading on carbon of 13.4 wt%, having a particle size of 3.2 nm. This preparation method could be valid also for the achievement of Pd–Pt/C catalysts with small particle size in more severe conditions, that is, Pd/Pt atomic ratio > 1 and metal loading of 20 wt%.

Palladium-based electrocatalysts have been tested as anode materials for alcohol oxidation in alkaline direct alcohol fuel cells [29]. In this work we have tested single PEMFCs with Pd-based electrodes, that is, a Pd catalyst with a very low Pt content (5 at.% Pt) as anode material, and a Pt-free Pd–Co and ternary Pd–Pt–Co catalysts as cathode materials. The performance of the best Pd-based PEMFC was compared with that of a PEMFC with conventional Pt electrodes.

2. Experimental part

2.1. Synthesis methods

Carbon supported Pt, Pd–Pt in the nominal atomic composition 95:5, Pd–Co (75:25) and Pd–Pt–Co (50:30:20) catalysts were prepared by reduction of metal precursors with formic acid. An appropriate amount of carbon powder (Vulcan XC-72, Cabot, 240 $m^2\,g^{-1}$) was suspended in 2 M formic acid solution and the suspension heated to 80 °C. Chloroplatinic acid ($H_2PtCl_6{\cdot}6H_2O$, Johnson Matthey) solution (in the case of Pt/C, Pd–Pt/C and Pd–Pt–Co/C), a palladium chloride ($PdCl_2{\cdot}2H_2O$, MERCK) solution (in the case of Pd–Co/C, Pd–Pt/C and Pd–Pt–Co/C) and cobalt nitrate ($Co(NO_3)_2{\cdot}6H_2O$, Aldrich) (for Pd–Co/C and Pd–Pt–Co/C) were slowly added to the carbon suspension. The suspension was left to cool at room temperature and the solid filtered and dried in an oven at 80 °C for 1 h. The material was 20 wt% metal on carbon. The Pd–Pt–Co/C catalysts in the nominal atomic ratio Pd:Pt:Co 50:30:20 were prepared by two ways: (1) simultaneous impregnation of Pd, Pt and Co precursors on the formic acid impregnated carbon support (catalyst named PdPtCoS), and (2) impregnation of Pd and Pt precursors on the support, then impregnation of Co, followed by thermal treatment at 700 °C under flowing N_2 (catalyst named PdPtCoT).

2.2. Structural characterization

The atomic ratio of the catalysts was determined by the energy dispersive X-ray (EDX) technique coupled to a scanning electron microscopy LEO Mod. 440 with a silicon detector with Be window and applying 20 keV.

X-ray diffractograms (XRD) of the electrocatalysts were obtained in a universal diffractometer Carl Zeiss-Jena, URD-6, operating with Cu k_α radiation (λ = 0.15406 nm) generated at 40 kV and 20 mA. Scans were done at 3° min^{-1} for 2θ values between 20° and 100°. It has to be remarked that the XRD measurements on as-prepared and thermally treated catalysts were carried out on the catalyst powder, whereas the XRD analysis on the catalysts submitted to RPC was carried out on the electrode.

The in situ X-ray absorption spectroscopy (XAS) measurements were performed in the Pt L_{III} absorption edges at 0.8 V *vs.* the reversible hydrogen electrode (RHE), using a spectro-electrochemical cell [22]. The working electrodes consisted of pellets formed with the dispersed catalysts agglutinated with PTFE (*ca.* 40 wt%) and containing 6 mg cm^{-2} of catalyst. The counter electrode was a Pt screen. This electrode was cut in the center, in order to allow the free passage of the X-ray beam. Prior to the experiments, the working electrodes were soaked in the electrolyte for at least 48 h. XAS experiments were made at 0.8 V *vs.* RHE, after cycling the electrodes in the range defined by these potentials. Results presented here correspond to the average of at least two independent measurements.

All the XAS experiments were conducted at the D04B-XAS1 beam line in the Brazilian Synchrotron Light Laboratory (LNLS), Brazil. The data acquisition system for XAS comprised three ionization detectors (incidence I_0, transmision I_t and reference I_r). The reference channel was employed primarily for internal calibration of the edge positions by using a foil of the pure metal. Nitrogen was used in the I_0, I_t and I_r chambers.Transmission electron micrograph (TEM) analysis was carried out at 120 kV using a JEOL JSM-5900LV microscope.

2.3. Electrochemical characterization

Tests in PEMFCs: For the PEMFC studies, the electrodes were hot pressed on both sides of a Nafion® 115 membrane at 125 °C and 50 kg cm^{-2} for 2 min. The Nafion® membranes were pre-treated with a 3 wt% solution of H_2O_2, washed and then treated with a 0.5 M solution of H_2SO_4. The geometric area of the electrodes was 4.6 cm^2. The metal loading was 0.4 mg cm^{-2} both at the anode and at the cathode. The Pt/C and Pd–Pt/C (95:5) samples were tested as anode catalysts, using a commercial 20 wt% Pt/C by E-TEK as the cathode catalyst. The Pd–Co/C, Pd–Pt–Co/C and Pt/C catalysts were tested as cathode materials, using the Pd–Pt/C (95:5) sample as the anode catalyst.

The polarization experiments in the PEMFC were carried out galvanostatically (Electronic Load HP 6050A) with the cell at 90 °C,

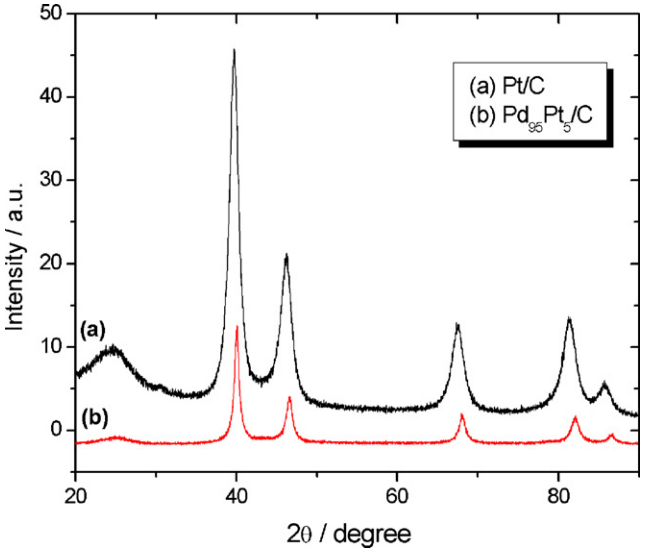

Fig. 1. XRD diffractograms of $Pd_{95}Pt_5/C$ and Pt/C catalysts.

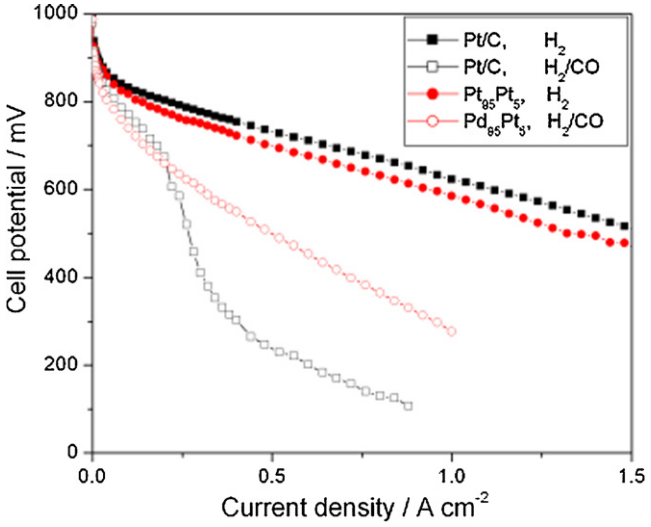

Fig. 2. Polarization curves in single PEMFCs operating at 90 °C and 3 atm O_2 pressure with $Pd_{96}Pt_4/C$ and Pt/C as anode electrocatalysts. Cathode: 20 wt% Pt/C. Anode and cathode metal loading 0.4 mg cm^{-2}.

using O_2 saturated with water at 90 °C and 3 atm in the cathode, and either pure hydrogen or a mixture of H_2/100 ppm CO saturated with water at 95 °C and 1 atm in the anode. The gases were primary mixture of 100 ppm carbon monoxide in hydrogen balance, nitrogen (99.996%), carbon monoxide (99.5%) and hydrogen or oxygen, all from White Martins. Before cell test, to activate the catalysts, the electrodes have been submitted to a repetitive potential cycling (1500 cycles) in the range 0.5–1.0 V. The cell polarization data were collected at 90 °C/3 atm O_2 pressure.

CO stripping experiments were performed on the gas diffusion electrodes using a potentiostat–galvanostat (Solartron 1285). In these experiments, the cathode was used as the working electrode, while the anode was used as both the counter and the RHE. The CO stripping experiments were carried out in the following way: after recording a CV in a N_2 purged system, CO was admitted to the cell and adsorbed at 0.075 V for 20 min. The excess CO was eliminated with N_2 gas and the stripping charges determined between 0.075 and 1.0 V *vs.* RHE using a scan rate of 10 mV s^{-1} after correcting the currents for the background. Being the $Pd_{49}Pt_{47}Co_4$ used as cathode catalyst, CO was bubbled only on the cathode. Linear sweep curves were recorded in the range 0.1–1.0 V *vs.* RHE.

3. Results

3.1. Pd-based anode catalysts

A PEMFC using a Pd–Pt/C catalyst with a very low Pt content as anode material was compared with a cell using a conventional Pt/C catalyst as anode material. As reported by Papageorgopoulos et al. [7] and Garcia et al. [8], the performance of Pd/C for the HOR as anode catalyst in PEMFC is very poor. For this reason we have chosen the nominal Pd:Pt composition 95:5. The value of Pd:Pt atomic ratio of the Pd–Pt/C catalyst was 96:4, near to the nominal composition. Fig. 1 shows the XRD patterns of the carbon supported Pd–Pt and Pt electrocatalysts. The lattice parameters and the particle size of these catalysts are given in Table 1. The value of the lattice parameter (0.3894 nm, slightly higher than that of pure Pd (a = 0.3890 nm)) indicates the formation of a PdPt alloy. The particle size of the Pd–Pt/C catalyst was more than twice with respect to Pt/C. Fig. 2 shows the current–potential curves for single PEMFCs using as anode materials the $Pd_{96}Pt_4/C$ and Pt/C catalysts, and conventional Pt/C as cathode material. As can be seen in Fig. 2, in agreement with previous works [8,9], the presence of a small amount of Pt remarkably increased the activity of Pd, attaining the value of pure Pt. The slightly lower performance of the cell with $Pd_{95}Pt_5/C$ as anode catalyst than that of the PEMFC with Pt/C could be ascribed to the higher particle size of the Pd-based catalyst than Pt. Moreover, as expected, $Pd_{95}Pt_5/C$ presented a higher CO tolerance than Pt/C.

3.2. Pd-based cathode catalysts

A Pt-free Pd–Co/C and ternary Pd–Pt–Co/C catalysts have been used as cathode materials in PEMFCs and compared with a conventional Pt/C. The EDX compositions of Pd–Co/C and Pd–Pt–Co/C catalysts are reported in Table 1. The amount of Pt in the PdPtCoS catalyst was lower than the nominal one, as well as the amount of Co in the PdPtCoT catalyst. Fig. 3 shows the XRD patterns of the carbon supported Pd–Co/C, Pd–Pt–Co/C and Pt/C electrocatalysts, and the lattice parameters and the crystallite size of these catalysts are given in Table 1. Assuming that the lattice parameter of PdPt alloys obey to Vegard's law in the entire range of compositions

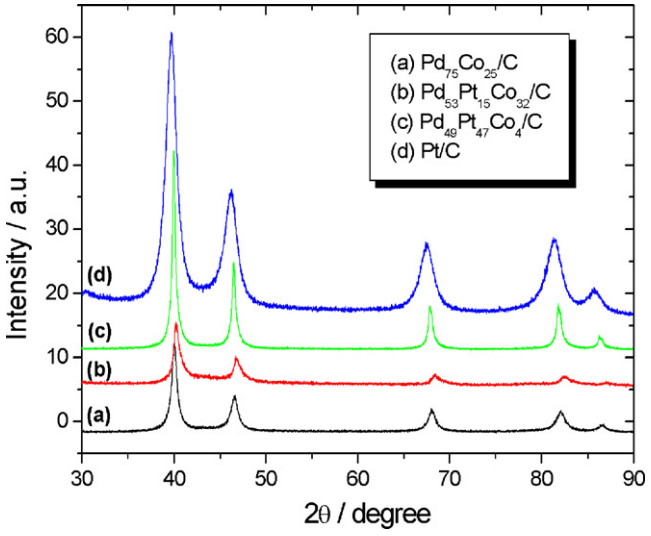

Fig. 3. XRD diffractograms of $Pd_{75}Co_{25}/C$, $Pd_{53}Pt_{15}Co_{32}/C$, $Pd_{49}Pt_{47}Co_4/C$ and Pt/C catalysts.

Table 1
EDX composition, lattice parameter, crystallite size by XRD and particle size by TEM of Pd–Co/C, Pd–Pt–Co/C and Pt/C catalysts.

Catalyst	EDX composition Pd:Pt:Co	Lattice parameter (2 2 0) (nm)	Particle size by XRD (2 2 0) (nm)	Particle size by TEM (nm)
Pt/C	0:100:0	0.3922	4.1	d_n 4.4 d_v 5.2
PdPtCoT/C (50:30:20)	49:47:4	0.3905	18	d_n 7.7 d_v 15* (without the particle with size 53 nm)
PdPtCoS/C (50:30:20)	53:15:32	0.3879	9.2	
$Pd_{75}Co_{25}$/C	75:0:25	0.3894	12.0	
$Pd_{95}Pt_5$/C	96:4:0	0.3894	11.3	

from pure Pt to pure Pd, we have calculated the lattice parameter of a PdPt alloy in the Pd:Pt composition = 1:1, *ca.* the Pd:Pt composition in the PdPtCoT catalyst. The calculated lattice parameter (0.3908 nm) was in good agreement with that experimental value of PdPtCoT (0.3905 nm). Co likely do not alloy or its effect on the lattice parameter is negligible due to its low amount. The lattice parameter of the PdPtCoS catalyst, instead, was lower than that calculated applying Vegard's law to the PdPt alloy in the Pd:Pt composition = 3.5:1, that is, the Pd:Pt atomic ration in the PdPtCoS catalyst. This means that likely a ternary PdPtCo alloy was formed. The very large particle size of the PdPtCoT/C catalyst is due to the thermal treatment at 700 °C. As the thermal treatment at 700 °C has been carried out under flowing N_2, cobalt is present in the reduced form Co(0).

Fig. 4 shows the current–potential and power density curves for a single PEMFC using as cathode materials the activated $Pd_{75}Co_{25}$/C, PdPtCoS/C, PdPtCoT/C and Pt/C catalysts, and the $Pd_{96}Pt_4$/C catalyst as anode material. The cathode performance was in the order Pt/C > PdPtCoT/C > PdPtCoS/C ≫ $Pd_{75}Co_{25}$/C. The performance of the Pt-free $Pd_{75}Co_{25}$/C was poor: the maximum power density (MPD) of the cell with Pd75Co25/C as cathode catalyst was 25% of MPD of the cell with Pt/C as cathode material. The cell with PdPtCoT/C as cathode catalyst, instead, showed a good performance, with a value of MPD which attained 85% of that of the cell with Pt/C as cathode catalyst. In a fuel cell, the potential at 0.01 mA cm^{-2}, $V_{0.01}$, is a useful parameter to evaluate the ORR activity [30]. Fig. 5 shows the dependence of $V_{0.01}$ on Pt content in the catalyst. The data follow a parabolic law with a maximum for a Pt content of *ca.* 70%, in agreement with the literature results [17,21].

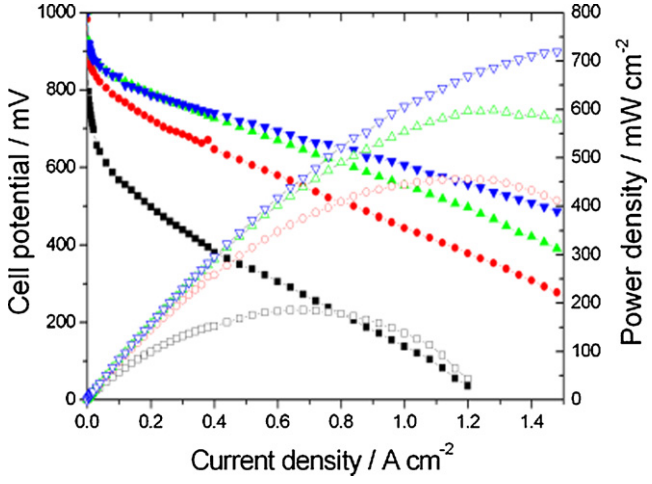

Fig. 4. Polarization and power density curves in single PEMFCs operating at 90 °C and 3 atm O_2 pressure with $Pd_{75}Co_{25}$/C (squares), PdPtCoS/C (circles), PdPtCoT/C (up triangles) and Pt/C (down triangles) as cathode electrocatalysts. Full symbols: polarization data; open symbols: power density data. Anode: 20 wt% $Pd_{96}Pt_4$/C. Anode and cathode: catalyst loading 0.4 mg cm^{-2}.

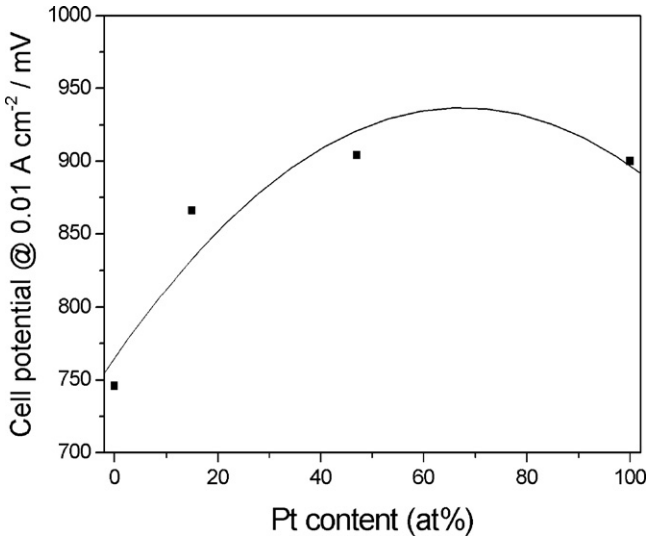

Fig. 5. Dependence of the PEMFC potential at 0.01 A cm^{-2} on Pt content in the catalyst.

3.2.1. *Comparison of structural characteristics of $Pd_{49}Pt_{47}Co_4$/C and Pt/C*

Among the catalysts tested as cathode material in PEMFCs, PdPtCoT/C was the most interesting, so we have investigated more in detail its characteristics and compared with those of Pt/C.

Fig. 6 shows the X-ray absorption near edge structure (XANES) spectra at the Pt L_3 edge at 0.8 V *vs.* RHE for the as-prepared PdPtCoT/C and Pt/C electrocatalysts, and for the reference Pt foil. A

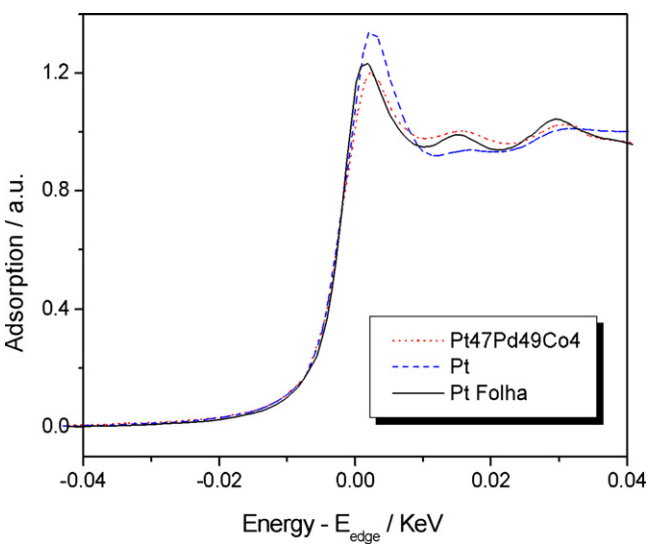

Fig. 6. Pt L_3 XANES spectra at 0.8 V *vs.* RHE for carbon supported Pt and PtPdCoT electrocatalysts relative to a Pt reference foil in 0.5 mol L^{-1} H_2SO_4.

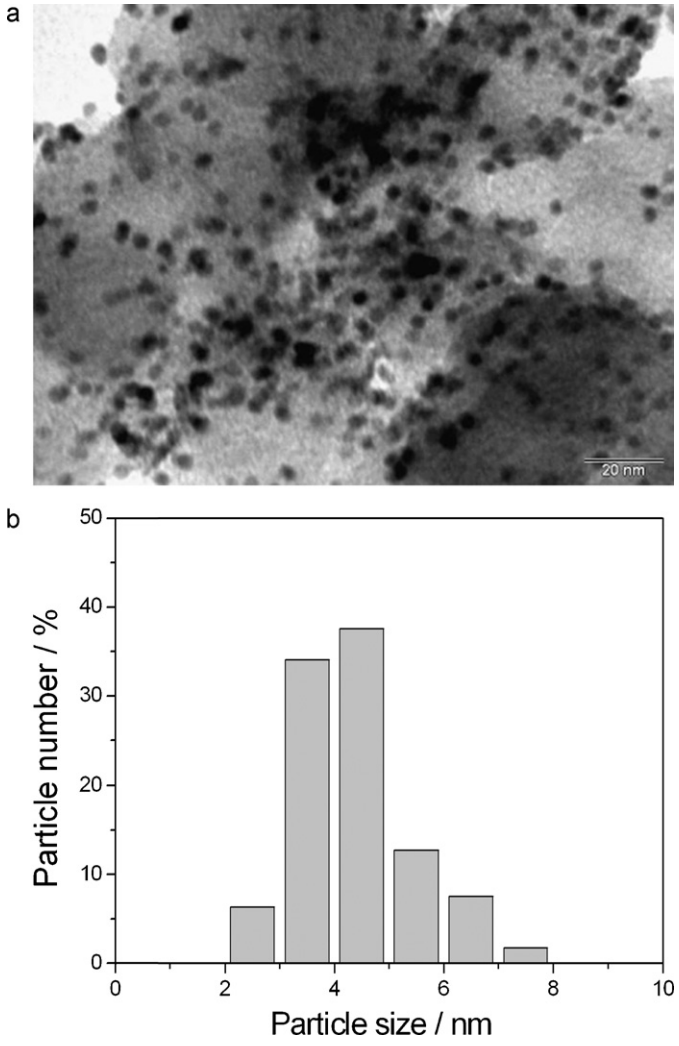

Fig. 7. TEM image (a) and histogram of particle size distribution (b) of the Pt/C catalyst.

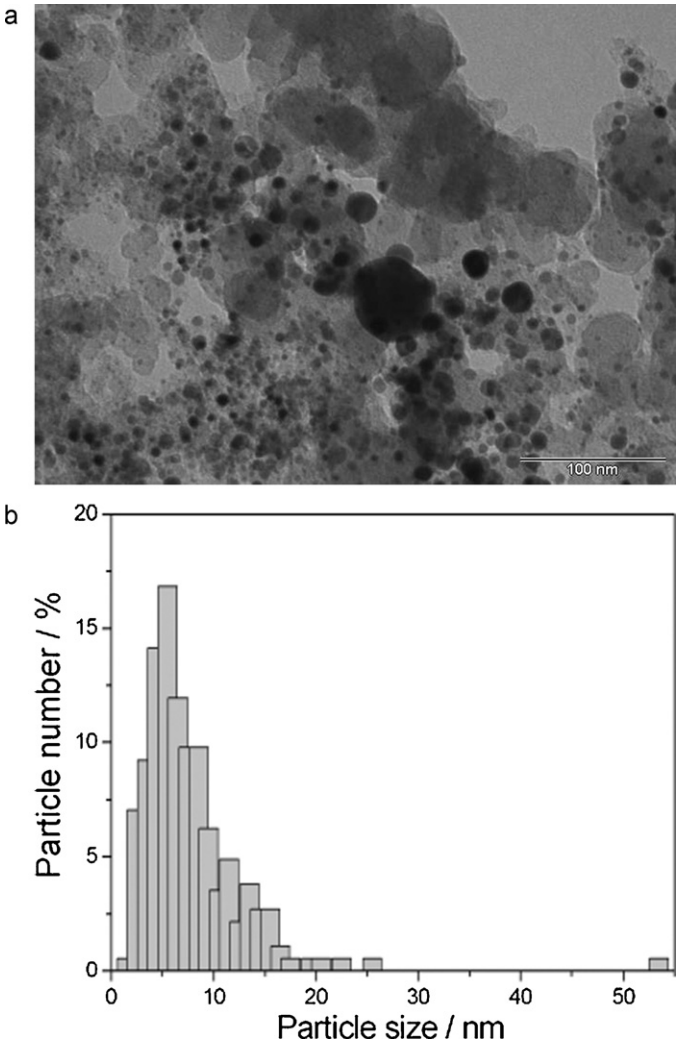

Fig. 8. TEM image (a) and histogram of particle size distribution (b) of the PdPtCoT/C catalyst.

significant increase in the intensity of the Pt L_3 white line of Pt/C compared to PdPtCoT/C and the reference Pt foil was observed. Normally, the intensity of the Pt L_3 edge increases with the increase in Pt d-band vacancy, in this case due to the adsorption of oxygenated species [31]. The affinity of OH chemisorption on Pt depends on both the metal particle size and alloying. It is known that there is an increase in the affinity of OH chemisorption on Pt as the metal particle size decreases [32] and the amount of M in Pt–M also decrease in Pt alloys [31]. The lower intensity of the Pt L_3 white line of PdPtCoT/C compared to that of Pt/C was mainly due to the higher particle size of PdPtCoT/C than Pt/C, but also to alloying effect.

Figs. 7 and 8 show the results of TEM analysis of the as-prepared Pt/C (Fig. 7) and PdPtCo/C (Fig. 8) catalysts. As can be seen in Fig. 7a, the distribution of Pt particles on the carbon support is in a narrow particle size range. The histogram of the particle size distribution (Fig. 7b) reflects quantitatively the size distribution in the Pt/C catalyst, with a narrow particle distribution centered at a particle size of 4.5 nm. Conversely, the image of the PdPtCoT/C catalyst (Fig. 8a) shows a non-uniform distribution of the particle size, with the presence of some giant particles (size > 30 nm) together with particles having a smaller size and in a narrow particle size range. The histogram of the PdPtCoT/C (Fig. 8b) shows a wide particle distribution, with the presence of a tail at large particles, with one particle large than 50 nm, likely formed during the thermal treatment.

The number averaged particle size, d_n, and the volume averaged particle size, d_v, have been calculated using Eqs. (1) and (2):

$$d_n = \frac{\sum(k) n_k d_k}{\sum(k) n_k} \quad (1)$$

$$d_v = \frac{\sum(k) n_k d_k^4}{\sum(k) n_k d_k^3} \quad (2)$$

where n_k is the frequency of occurrence of particles with size d_k. The particle sizes of Pt/C obtained from the TEM images were in agreement with those calculated from the XRD (2 2 0) peak, as reported in Table 1, and the values of d_n and d_v were similar. In the case of the PdPtCoT/C catalyst, the discrepancy of the number averaged size by TEM with the crystallite size by XRD is due to the fact that the Scherrer formula yields a volume averaged size, to which the largest particles contribute disproportionately. The higher value of d_v than that of d_n confirms the effect of the large particles on the main particle size. The chemical surface area (CSA) of the metal particles was calculated using the following equation:

$$\mathrm{CSA}\,(\mathrm{m^2\,g^{-1}}) = \frac{6 \times 10^3}{\rho d_n} \quad (3)$$

where ρ is the density of Pt (21.4 g cm^{-3}) or the Pd–Pt (1:1) alloy (16.8 g cm^{-3}). The values of CSA are reported in Table 2.

Table 2
Chemical surface area (CSA) and electrochemical surface area (ECSA) of PdPtCoT/C and Pt/C, and potential at 0.01 A cm^{-2} ($\Delta V_{0.01}$) and maximum power density (MPD), in terms of both geometric area and ECSA, of PEMFCs with PdPtCoT/C and Pt/C as cathode catalysts.

Catalyst	CSA (TEM) (m^2 g^{-1})	ECSA (CO stripping) (m^2 g^{-1})	$\Delta V_{0.01}$ (mV)	MPD (geometric area) (mW cm^{-2})	MPD (ECSA) (mW cm^{-2})
PdPtCoT/C	46.4	35.6	904	598	4.2
Pt/C	63.7	48.5	900	710	3.7

Fig. 9 shows the results of the linear sweep CO stripping experiments. In agreement with the results of Garcia et al. [8], the peak potential for PdPtCoT/C occurred at a higher value than for Pt/C, indicative of the stronger CO bonding to Pd. While CO adsorption on PtPdCoT/C can occur on both Pt and Pd atoms, the oxidation involves only a single uniform peak. A synergistic effect is thus evident; the peak is not simply an addition of fractional contributions of Pt and Pd sites. Electronic modification of the CO adsorption characteristics on the two metals, due to alloy formation, is clearly supported by the results shown in Fig. 9. The electrochemical chemical surface area (ECSA) of the metal particles obtained by CO stripping is reported in Table 2. From the electrochemical surface area (ECSA, by CO stripping) and the chemical surface area (CSA, by TEM) the Pt utilization efficiency, i.e. the ratio between the ECSA and CSA, can be calculated [33,34]. The catalyst utilization efficiency was similar, 0.76 and 0.77 for Pt/C and PdPtCoT/C, respectively, in agreement with the value of 0.72 reported in the literature [33,34]. As shown in Table 2, the PdPtCoT/C catalyst presented a specific activity, in terms of $V_{0.01}$, slightly higher than that of Pt/C. In agreement with the values of $V_{0.01}$, while the MPD of the cell with PdPtCoT/C, expressed in terms of the geometric area, that is, in terms of mass activity, is lower than that of the cell with Pt/C, the MPD of the PEMFC with PdPtCoT/C, expressed in terms of the electrochemical surface area, that is, in terms of specific activity, is slightly higher than that of the cell with Pt/C (see Table 2).

3.3. Comparison of PEMFCs with Pd-based and conventional Pt electrodes

The polarization and power density curves of PEMFCs with $Pd_{96}Pt_4$/C and PtPdCoT/C as anode and cathode catalysts, respectively, and with conventional Pt/C catalysts are shown in Fig. 10. As can be seen in Fig. 10, the performance of the cell with Pd-based electrodes was only slightly lower than that of the cell with conventional Pt/C electrodes. The power densities at 1 A cm^{-2} were 623 and 554 mW cm^{-2} for the cells with Pt/C and Pd-based catalysts, respectively. A performance loss of only 11% occurred, with 6% ascribed to the anode and 5% to the cathode. The maximum power density (MPD) of the Pd-based cell was 76% of the MPD of the cell with Pt/C catalysts. The lower performance has to be ascribed to the higher particle size of both the Pd-based anode and cathode catalysts than Pt/C.

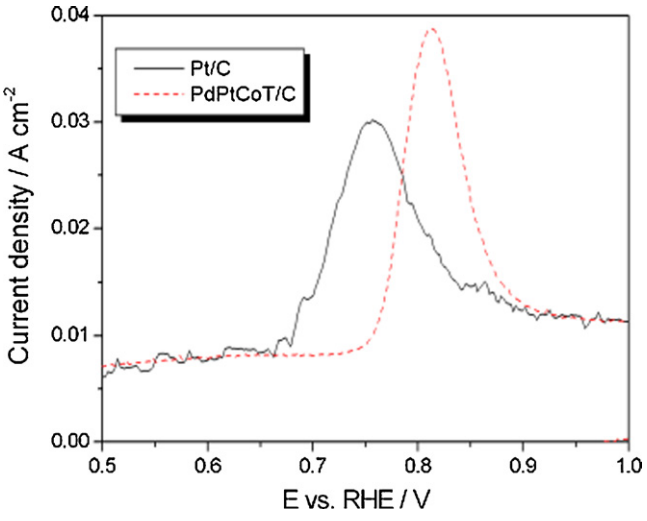

Fig. 9. CO_{ads} stripping voltammograms of Pt/C and PdPtCoT/C electrocatalysts.

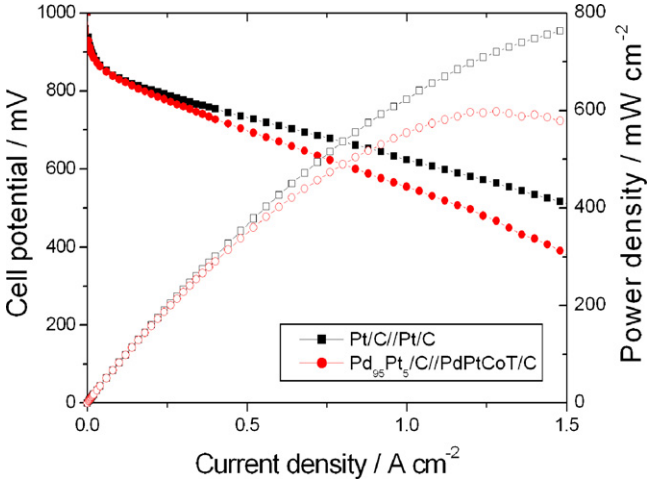

Fig. 10. Polarization and power density curves of single PEMFCs operating at 90 °C and 3 atm O_2 pressure with $Pd_{96}Pt_4$/C and $Pd_{49}Pt_{47}Co_4$/C as anode and cathode catalysts, respectively, and with conventional Pt/C catalysts. Full symbols: polarization data; open symbols: power density data. Anode and cathode: catalyst loading 0.4 mg cm^{-2}.

4. Conclusions

The performances of PEMFCs with Pd-based catalysts were compared with that of a PEMFC with conventional Pt/C catalysts. The power density at 1 A cm^{-2} of a cell with $Pd_{96}Pt_4$/C and Pt/C as anode and cathode catalysts, respectively, was only slightly lower (94%) with respect to the conventional PEMFC with Pt/C catalysts at both electrodes. The performance at 1 A cm^{-2} of a quasi Pt-free PEMFC with $Pd_{96}Pt_4$/C as anode catalyst and $Pd_{75}Co_{25}$/C as cathode catalyst (overall Pd:Pt:Co catalyst composition 85.5:2:12.5), instead, was considerably lower (22%) than that of the cell with Pt/C catalysts. Finally, the performance at 1 A cm^{-2} of a PEMFC with $Pd_{96}Pt_4$/C as anode catalyst and PdPtCoT/C as cathode catalyst (overall Pd:Pt:Co catalyst composition 72:26:2) was 89% than that of the conventional PEMFC, with a performance loss of 6% ascribed to the anode catalysts and 5% to the cathode catalyst. Thus, this work demonstrates that Pd-based catalysts can substitute conventional Pt catalysts in PEMFCs with only a slightly loss in cell performance, particularly at high current densities. For both electrodes, the performance loss is due to the higher particle size of Pd-based catalysts than Pt, decreasing the active surface area of the catalyst, and negatively influencing their catalytic activity. To reduce cell performance loss, it is necessary to synthesize Pd-based catalysts with low particle size. So, further works should be addressed to develop new synthesis methods of Pd-based catalysts with low Pt content and low particle size, maintaining a high catalytic activity.

Acknowledgment

The authors thank the Conselho Nacional de Desenvolvimento Científico e Tecnológico (CNPq, Proc. 310151/2008-2) for financial assistance to the project.

References

[1] A.T. Haug, R.E. White, J.W. Weidner, W. Huang, S. Shi, T. Stoner, N. Rana, J. Electrochem. Soc. 149 (2002) A280.
[2] J.-H. Wee, K.-Y. Lee, S.H. Kim, J. Power Sources 165 (2007) 667.
[3] E. Antolini, Energy Environ. Sci. 2 (2009) 915.
[4] M. Maximov, O.A. Petrii, Elektrokhimiya 10 (1974) 1721.
[5] M.S. Rau, P.M. Quaino, M.R.G. de Chialvo, A.C. Chialvo, Electrochem. Commun. 10 (2008) 208.
[6] J.J. Salvador-Pascual, S. Citalán-Cigarroa, O. Solorza-Feria, J. Power Sources 172 (2007) 229.
[7] D.C. Papageorgopoulos, M. Keijzer, J.B.J. Veldhuis, F.A. De Bruijn, J. Electrochem. Soc. 149 (2002) A1400.
[8] A.C. Garcia, V.A. Paganin, E.A. Ticianelli, Electrochim. Acta 53 (2008) 4309.
[9] Y.-H. Cho, B. Choi, Y.-H. Cho, H.-S. Park, Y.-E. Sung, Electrochem. Commun. 9 (2007) 378.
[10] J.L. Fernandez, D.A. Walsh, A.J. Bard, J. Am. Chem. Soc. 127 (2005) 357.
[11] M.H. Shao, T. Huang, P. Liu, J. Zhang, K. Sasaki, M.B. Vukmirovic, R.R. Adzic, Langmuir 22 (2006) 10409.
[12] M.-H. Shao, K. Sasaki, R.R. Adzic, J. Am. Chem. Soc. 128 (2006) 3526.
[13] S. Song, Y. Wang, P. Tsiakaras, P.K. Shen, Appl. Catal. B 78 (2008) 381.
[14] V. Raghuveer, P.J. Ferreira, A. Manthiram, Electrochem. Commun. 8 (2006) 807.
[15] W. Wang, D. Zheng, C. Du, Z. Zou, X. Zhang, B. Xia, H. Yang, D.L. Akins, J. Power Sources 167 (2007) 243.
[16] H. Liu, A. Manthiram, Energy Environ. Sci. 2 (2009) 124.
[17] H. Li, G. Sun, N. Li, S. Sun, D. Su, Q. Xin, J. Phys. Chem. C 111 (2007) 5605.
[18] T. Lopes, E. Antolini, E.R. Gonzalez, Int. J. Hydrogen Energy 33 (2008) 5563.
[19] J. Yang, J.Y. Lee, Q. Zhang, W. Zhou, Z.L. Yang, J. Electrochem. Soc. 155 (2008) B776.
[20] Y. Xu, X. Lin, J. Power Sources 170 (2007) 13.
[21] S. Guerin, B.E. Hayden, C.E. Lee, C. Mormiche, A.E. Russell, J. Phys. Chem. B 110 (2006) 14355.
[22] H. Ye, R.M. Crooks, J. Am. Chem. Soc. 129 (2007) 3627.
[23] M. Ohashi, K.D. Beard, S. Ma, D.A. Blom, J. St-Pierre, J.W. Van Zee, J.R. Monnier, Electrochim. Acta 55 (2010) 7376.
[24] S.A. Grigoriev, E.K. Lyutikova, S. Martemianov, V.N. Fateev, Int. J. Hydrogen Energy 32 (2007) 4438.
[25] Z. Liu, L. Hong, M.P. Tham, T.H. Lim, H. Jiang, J. Power Sources 161 (2006) 831.
[26] W. Wang, Q. Huang, J. Liu, Z. Zou, Z. Li, H. Yang, Electrochem. Commun. 10 (2008) 1396.
[27] J.B. Joo, Y.J. Kim, W. Kim, N.D. Kim, P. Kim, Y. Kim, J. Yi, Korean J. Chem. Eng. 25 (2008) 770.
[28] K.D. Beard, J.W. Van Zee, J.R. Monnier, Appl. Catal. B: Environ. 88 (2009) 185.
[29] C. Bianchini, P.K. Shen, Chem. Rev. 109 (2009) 4183.
[30] S. Mukerjee, S. Srinivasan, M.P. Soriaga, J. Electrochem. Soc. 142 (1995) 1409.
[31] S. Mukerjee, S. Srinivasan, M.P. Soriaga, J. McBreen, J. Phys. Chem. 99 (1995) 4577.
[32] S. Mukerjee, J. McBreen, J. Electroanal. Chem. 448 (1998) 163.
[33] W. Li, W. Zhou, H. Li, Z. Zhou, B. Zhou, G. Sun, Q. Xin, Electrochim. Acta 49 (2004) 1045.
[34] F. Colmati, E. Antolini, E.R. Gonzalez, Electrochim. Acta 50 (2005) 5496.